Reprinted from Preprint Volume: Tenth Conference on Severe Local Storms. Oct. 18-21, 1977; Omaha, NE. Published by American Meteorological Society, Boston, Massachusetts.

MESOANALYSIS OF RECORD CHICAGO RAINSTORM USING RADAR, SATELLITE, AND RAINGAUGE DATA

by

T. Theodore Fujita and Mark R. Hjelmfelt
The University of Chicago

and

Stanley A. Changnon
Illinois State Water Survey

1. INTRODUCTION

On June 13, 1976 the Chicago area was hit by an F4 tornado, followed by a record rainfall which paralyzed city streets and highways for hours. Two persons were killed by a tornado near Lemont and two more were flood-related victims in Chicago.

Shortly after 0000 Z flood water poured into the low sections of the Dan Ryan Expressway which extends south from the Downtown area. Sunday motorists who were not familiar with the neighborhood managed to drive out of the expressway, meeting street gangs who stoned or stopped their cars. A driver with his family in the car was shot to death.

Shown in Fig. 1 are isohyets for a 5-hour period, 2030 to 0130 GMT (330 to 830 PM CDT). There were three centers of heavy rainfall, as indicated by letters "a", "b", and "c". Over 5 to 7 inches of rainfall occurred at these locations. The flood water did not recede for several days at location "a" which was hit hardest.

Most underpasses were flooded at "b" where heavy rain occurred near the Tri-State Expressway (see Fig. 2). The third center, "c", was located away from population centers, resulting in only minor flood damage but heavy erosion in rural areas.

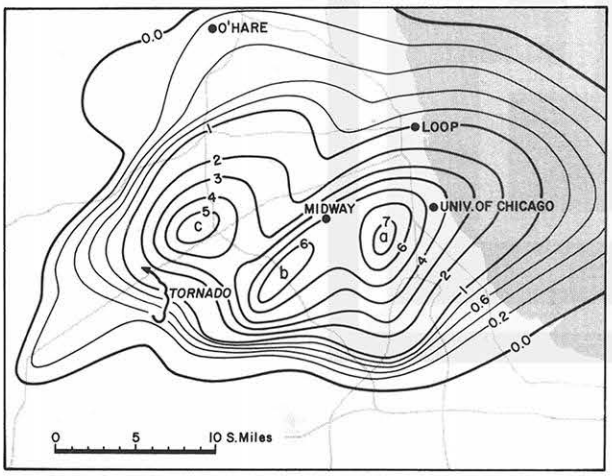

Fig. 1. Isohyets of the 5-hour period of Chicago rainstorm between 2030Z and 0130Z.

In addition to a severe F4 tornado and extremely heavy short-duration rains, this storm system produced exceptional, near record hailfalls. The first hail from the storm began at 2120 GMT and the last ended at 0130 GMT. Seventeen sites had hail that lasted for 20 or more minutes and near record numbers of moderate (2 cm) to large (3 to 4 cm) hailstones fell.

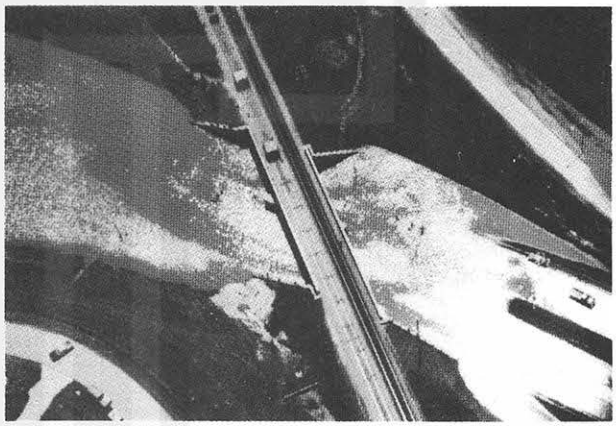

Fig. 2. Flooded underpass of a 4-lane divided highway at "b". Photo by Fujita on June 14, 1976.

A description of the unusual tornado produced by this storm has been given by Fujita (1976). This paper focuses on an interpretation of the unusually detailed surface rain and hail data available and on the associated radar and satellite data. These unique data permit an evaluation of airflow motions, which helped us to understand the mesoscale storm environment and to develop some findings relevant to the proper interpretation of radar and satellite data for severe storms. A careful comparative analysis of the satellite and radar data with the rain and hail data was used to 1) estimate the contribution of both hydrometeors to the reflectivity; 2) discern differences between precipitation rate and signal intensity so as to infer the presence and magnitude of vertical air motions; and 3) reveal how the mesoscale (storm related) and macroscale circulations interacted.

2. SATELLITE PICTURES

SMS pictures revealed that the rainstorm was an isolated cloud with an anvil extending eastward. The height of the anvil, estimated from its shadow, was about 32,000 ft where a stable layer existed according to the Peoria, Illinois sounding at 2300 Z. Winds aloft at this layer were 50 to 56 kts from 255°.

A band of wake cirrus extended downwind from the convective region. The cirrus cloud in the wake was characterized by a narrow band of shadow along its southern edge and a narrow bright band along the northern edge. The wake was 3 to 5,000 ft higher than the anvil top (see Figs. 3 and 4). For wake cirrus refer to Fujita (1974).

The Peoria sounding shows that winds above the stable layer were about 15 kts faster than those at the anvil top. Computed motion of the leading edges of the anvil and the wake cirrus revealed that the latter was 76 kts while the former was 61 kts (see Fig. 5).

Fig. 3. Anvil and wake cirrus at 2330 Z. Note that fast-moving wake cirrus generated horizontal shear at the anvil top, inducing a herringbone pattern.

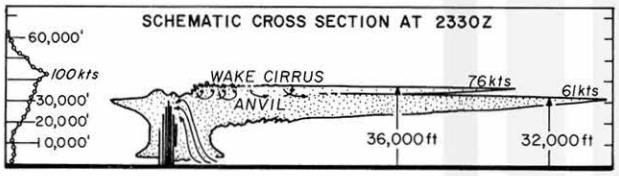

Fig. 4. Schematical vertical cross section of the rainstorm in Fig. 3. There was a stable layer at 32,000 ft beneath the tropopause at 44,000 ft.

It is obvious, therefore, that the wake cirrus moved eastward faster than the anvil cloud. As expected, the anvil cloud near the wake cirrus moved faster than its edge. Patterns of slanted parallel bands such as these may be called the "herringbone pattern".

In comparison with an extensive area of anvil cloud, the precipitation areas are extremely small. Shown in Fig. 6 are two areas of precipitation at 2215 Z when the Lemont tornado had touched down. The cloud was characterized by a wake cirrus in development stage as well as a herringbone anvil on the southern part of the anvil cloud.

At 2230 Z when the tornado was in its mature stage of F 4, the wake cirrus extended into southeastern Michigan. Contour lines denote isohyets of 0 and 1 in/hr rainfall rates (see Fig. 7).

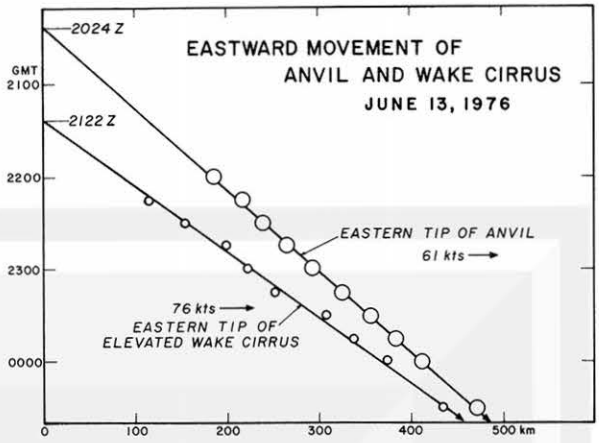

Fig. 5. Fast-moving wake cirrus above the anvil cloud. The anvil formed before wake cirrus did but the former was overtaken by the latter 5 hours later.

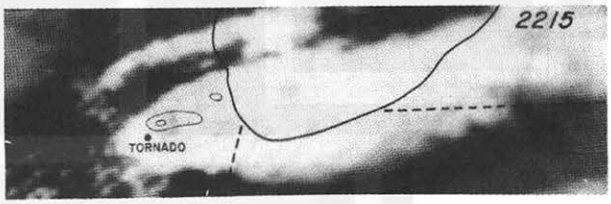

Fig. 6. Zero and one in/hr isohyets superimposed upon an SMS picture at 2215 Z (515 pm CDT) when the Lemont tornado touched down.

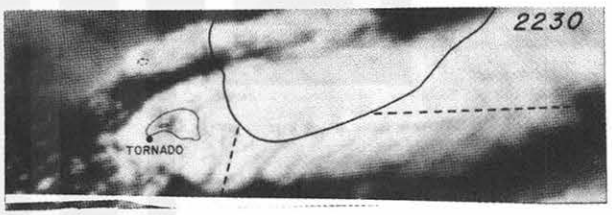

Fig. 7. Isohyets on satellite picture at 2230Z when the tornado reached the F 4 intensity.

One hour later at 2330 Z, precipitation cells in the Chicago area reached their mature stage. Isohyets of 3 to 4 in/hr are visible inside the precipitation area. The elevated wake cirrus is accompanied by herringbone patterns (see Fig. 8).

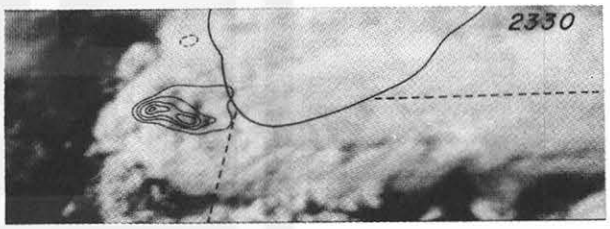

Fig. 8. Isohyets on satellite picture at 2330Z. Note herringbone patterns to the south of the wake cirrus.

In order to place isohyets at the anvil level above rainfall areas, geographic locations were computed by placing grids at the anvil height of 32,000 ft MSL. Both at 2230 and at 2330 Z, rainfall centers do not always coincide with brightness centers at the cloud top. Instead, some centers are located where

the cloud tops are dark, which indicates eastern slope or depression on anvil.

The heaviest rainfall center of 5 inches per hour at 0030 Z was located just to the north of the darkest spot of the anvil. Brightness centers are seen on both sides of rainfall centers, suggesting that we cannot relate brightness values with rainfall rates in mesoscale dimensions (see Fig. 9).

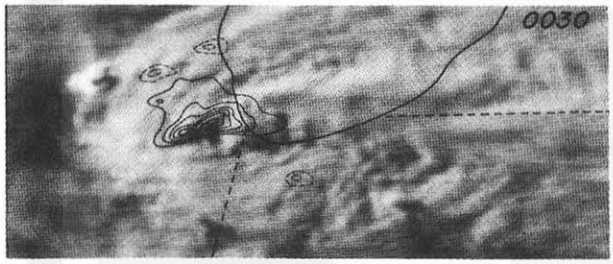

Fig. 9. Isohyets on satellite picture at 0030Z. Area of heavy rain was located near dark shadow regions atop the anvil.

3. RADAR ECHOES AND RAINFALL RATES

A raingauge network of the Illinois State Water Survey was put into operation just about one week in advance of the record rainstorm. The network consisting of weighing-bucket raingauges and hail pads covered the entire areas of the rainstorm.

The areas of rainfall were located near the 50 nautical mile range of the NWS Marseilles radar. At this distance the center of the radar beam was about 2 km above ground level. Radar pictures were taken at about 6-min intervals during the early period of the rainstorm. Later, intervals were reduced to about 1 min. For this case study, pictures were printed at 5 - 6-min intervals during 2200 Z - 0100 Z period when most precipitation occurred.

Radar pictures were recorded with contour steps which vary, grey - black - white - black - white. Since fractional steps can be estimated at any point in radar pictures, the following decimal steps were used in this paper.

Step 0 ... beginning of the grey area
Step 10 ... beginning of the first black area
Step 20 ... beginning of the first white area
Step 30 ... beginning of the second black area
Step 40 ... beginning of the second white area

In an attempt to compare time variations of contour steps and rainfall rates at each raingauge station, steps at each station were read off on every radar picture. Then the raingauge traces were differentiated with respect to time to obtain rainfall rate.

In order to record impact forces of hailstones, funnels for collecting rainwater had been removed. Traces, thus recorded impact of hailstones as well as wind gusts strong enough to shake the gauges.

Shown in Fig. 10 are time variations of contour steps, spikes of wind or hail, and rainfall rate in inches per hour. Time sections for all stations were completed first, for their use in further analyses.

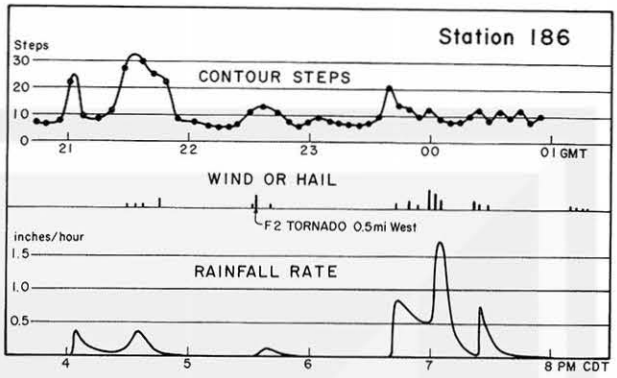

Fig. 10. Time variations of contour steps, rainfall rates, and hail or wind spikes at raingauge station No. 186.

4. ANALYSIS OF HAIL

Hail was reported from the areas of heavy rain. At the University of Chicago hail was observed for about 30 min while heavy rain was in progress. At Midway Airport hail was reported as follows: 2239 Z, hail began; 2242 Z, 1/8 inch hailstones; 2251 Z, 1/8 inch hailstones; 2316 Z, 1 inch hailstones; 2339 Z, hail ended. Total duration was 60 minutes.

Although no visual record of hail is available elsewhere, hail spikes on raingauge traces were used to make rough estimates of the hail period at each raingauge station (see Fig. 11).

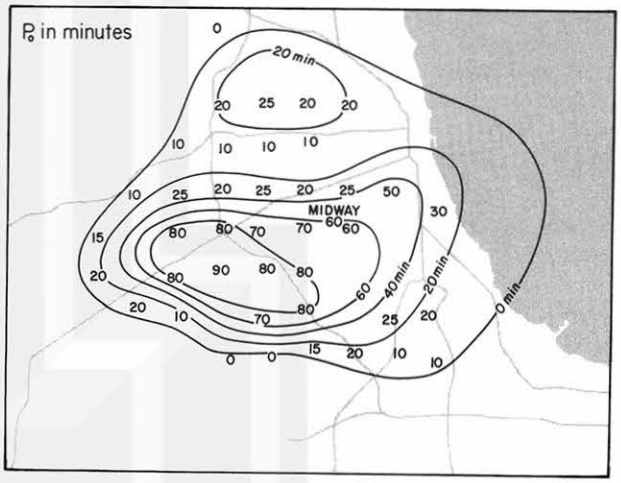

Fig. 11. Estimated periods of hail, 1/10 inch or larger.

The hailstorms of 13 June were near record events for hail from a single meso-storm system, based on several hail characteristics. The areal extent of hail in the 13 June storm covered 1080 km^2, which ranks it as the second most extensive hailfall observed in 6 years of storm study in Illinois (Changnon and Morgan, 1976). Hail fell repeatedly, averaging 3 different hailfalls at each site with up to 10 hailfalls at two sites. The total number

of hailstones was exceptional with more than 500 hailstones per square foot recorded over 450 km^2. Hailstones with diameters 2.2 cm or greater fell over 730 km^2 with the largest being 4 cm.

In general, most of the hail fell in the heavy rainfall cores and between 2300 to 0040 GMT. Hail kept developing in the central and western storm sections (rain cores b and c, Fig. 1); with hailcells enlarging as they moved slowly to the ESE.

5. RAINFALL RATES

The initial analysis of Z - R relationships based on reflectivity values interpolated from the step gain intervals did not produce a close correspondence. A better relationship was obtained by relating rainfall rate to the actual contour steps (each interval or step ranging from 6 to 12 DBZ).

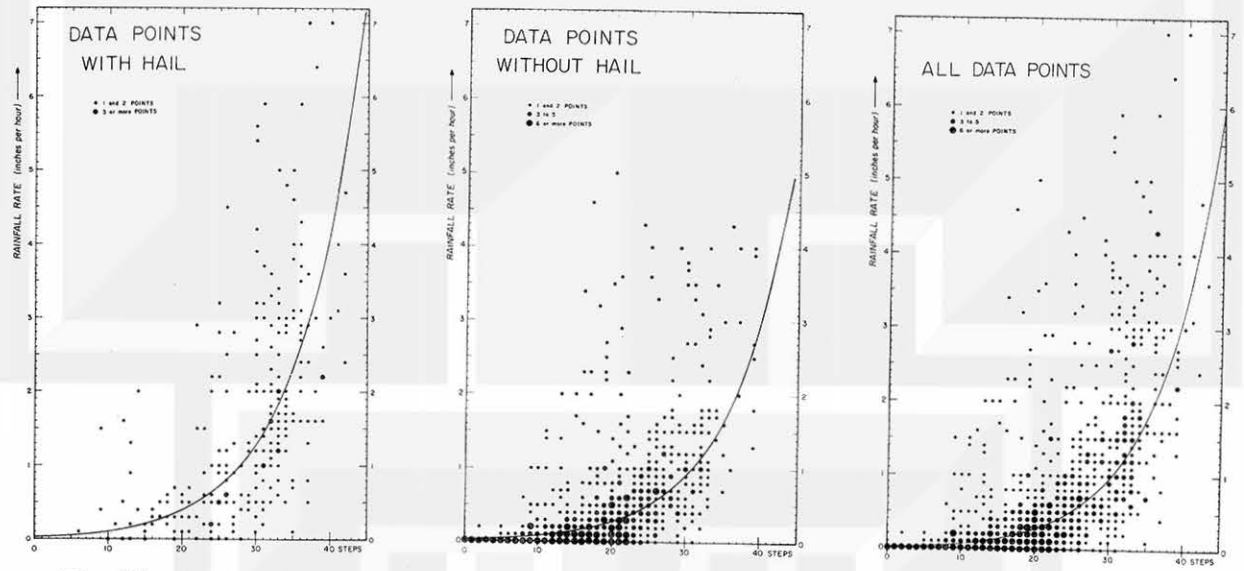

Fig. 12. Scatter diagrams showing contour step-rainfall rate (S-R) relationship. Data points with hail and without hail were plotted separately in left and center diagrams. Right diagram includes all data points.

In order to produce a data pair of contour step (S) and rainfall rate (R) at a given time and station we had to 1. position radar echoes precisely on the network map (echo of Downtown Chicago was used as a fixed target); 2. adjust rain recording time with radar time (time on and off plus minor adjustment); and 3. smooth rainfall rate to fit beam width of radar (3 to 5-min running average was applied).

Since it was expected that S - R data pair with hail is characterized by larger S than that without hail, data pairs were sorted into two categories, "with hail" and "without hail". They were then plotted into the three charts seen in Fig. 12.

Unexpectedly, S - R relationships "with hail and "without hail" turned out to be similar to each other. S - R with hail even shows slightly smaller S than those without hail.

Why is it that the presence of hail does not increase significantly the effective reflectivity? The only explanation we can offer at this time is "partial filling of radar beam by hail". The beam width (half-power) of the Marseilles radar of 2° and pulse duration of 4 μ sec imply a pulse volume over the heavy rain area of approximately 3.2 km (2 mi) by 600 m (0.4 mi).

The Chicago rainstorm was a "rainstorm with hail" rather than a "hailstorm with rain", from a radar standpoint. Isohyetal pattern during the height of the storm shows that the volume of heavy rain was often large enough to fill the radar beam. On the other hand, hail shafts were likely smaller than the heavy rain cores and thus the hail did not often fill the beam as well as the rain did (Changnon, 1968). It was considered reasonable, therefore, to put all S - R data pairs together to obtain the averaged S - R curve in Fig. 12.

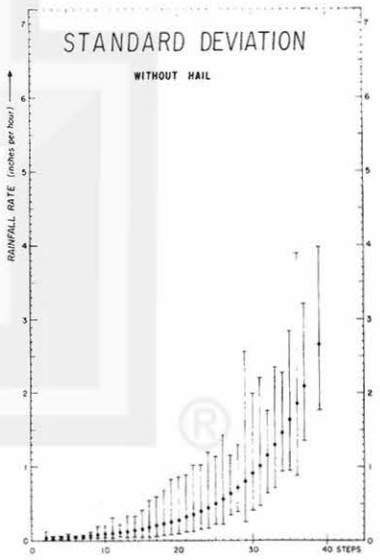

Fig. 13. Standard deviation of data points without hail.

In an attempt to estimate the scatter of data points, standard deviations were computed for each step, S. Results are presented in Fig. 13. Some rainfall rates were so large that we had to look further for explanations of these deviations.

6. EFFECTS OF VERTICAL VELOCITY

In an attempt to determine effects of up- and downdrafts upon R, rainfall rate, relationships with draft velocities were obtained assuming Marshall and Palmer (1948) type drop-size distributions and raindrop terminal velocities given by Gunn and Kinzer (1949).

An equation of terminal velocity was obtained by performing a curve fitting to the Gunn and Kinzer values. The equation obtained is

$$W_T = W_{MAX} \left(1 - e^{-6.6D} - 3De^{-14D} \right) \quad (1)$$

where W_{MAX} = 945 cm/sec. As shown in Fig. 14 terminal velocity, W_T is zero when D is zero and $W_T = W_{MAX}$ when D is infinity.

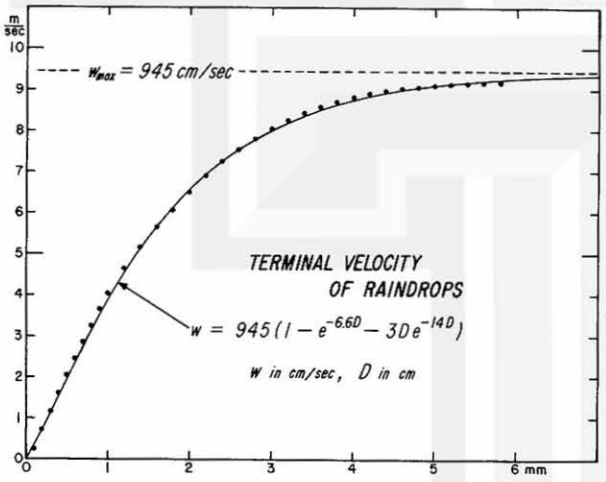

Fig. 14. Equation (1) obtained to fit terminal velocities by Gunn and Kinzer (1949).

The rainfall rate is computed from

$$R = \int_0^\infty \frac{\pi}{6} D^3 W_T N_0 e^{-\Lambda D} dD \quad (2)$$

where $\Lambda = 41 R^{-0.21}$, R in mm/hr, D in cm, and W_T in cm/sec. Since N_0 cannot be a constant in order to satisfy this equation, N_0 was computed from

$$N_0 = \frac{6R}{\pi \int_0^\infty D^3 W_T e^{-\Lambda D} dD} \quad (3)$$

Although an analytic solution of this equation is available, it can be approximated by

$$N_0 = 0.06 \left[1 + 0.2 R^{-1} + 0.57 (R+10)^{0.33} \right]. \quad (4)$$

By putting this value into Eq. (2) we are able to equate both sides with a high degree of accuracy. The resulting modification to the constant N_0 value of Marshall and Palmer of 0.08 is small with N_0 about 0.068 for small R and increasing to 0.08 at about 200 mm/hr. Some of the difference in N_0 from the Marshall and Palmer value is the result of use of the new fall speed relation.

Eq. (2) indicates the rainfall rate at the height of radar beam if there were no vertical motion of the air. An addition of draft velocities, either positive or negative, changes the rainfall rate on the ground because drops reach the raingauges at the speed of $W_R = W_T + W$, where W is the draft velocity and W_R, the fall velocity of raindrops relative to the surface.

The rainfall rate with draft velocity W is computed by

$$R_{(w)} = \frac{\pi N}{6} \int_{D_0}^\infty D^3 (W_T + W) e^{-\Lambda D} dD \quad (5)$$

where $R_{(w)}$ denotes rainfall rate under draft velocity, W, D_0, the drop diameter causing $W_R = 0$ in updraft. D_0 is zero in downdraft. In this computation we assume that the drop-size distribution at the beam height remains unchanged. It is the draft velocity beneath the beam which alters the fall velocity of raindrops relative to the ground.

Equation (5) reveals that a downdraft enhances the rainfall rate while an updraft suppresses or prevents surface rain. No rain will reach the surface when W_R is zero or smaller. This situation occurs when the updraft exceeds the maximum terminal velocity,

$$W_{MAX} = 945 \text{ cm/sec} \quad (6)$$

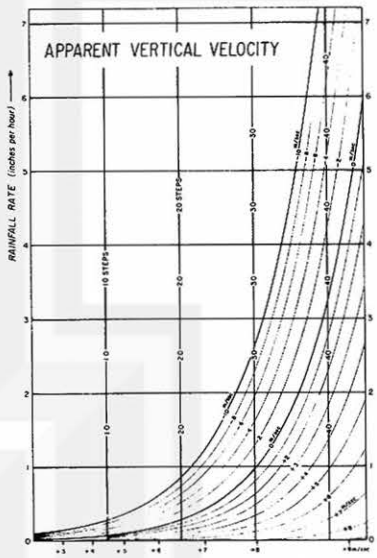

Fig. 15. Isolines of apparent vertical velocity computed from Eq. (5).

To determine the contribution of draft velocity upon rainfall rates, we assumed that

1. A Marshall-Palmer type drop size distribution is valid (thus effects of particle size sorting, etc., are not included).
2. No vertical motion exists when a data point is located on the averaged S - R line.

3. The draft velocity which shifts S - R line is called "apparent up- or downdraft".

4. Apparent draft velocity does not always represent "true draft velocity," but it is a measure of vertical motion fields.

Presented in Fig. 15 are isolines of "apparent draft velocities" computed from Eq. (5) by changing values between 10 m/sec and 9.45 m/sec.

7. EXAMPLES OF ANALYSES

Mesoscale analyses were performed for several situations. Those for 2216, 2231, 2330, and 0025 GMT are shown. Analyses charts include isohyets, stations with hail in progress, apparent draft velocities and estimated stream lines.

At 2216 Z the center of isohyets was located over the reflectivity center. Heavy rain was falling through zero apparent updraft, suggesting that the rain core did not produce a rushing downdraft. Argonne temperature was that of warm air while wind was coming from the rain core area. The northeast sector of a mesocyclone was characterized by an apparent updraft. The Lemont tornado touched down to the west of the mesocyclone center where cyclonic vorticity is expected to be large.

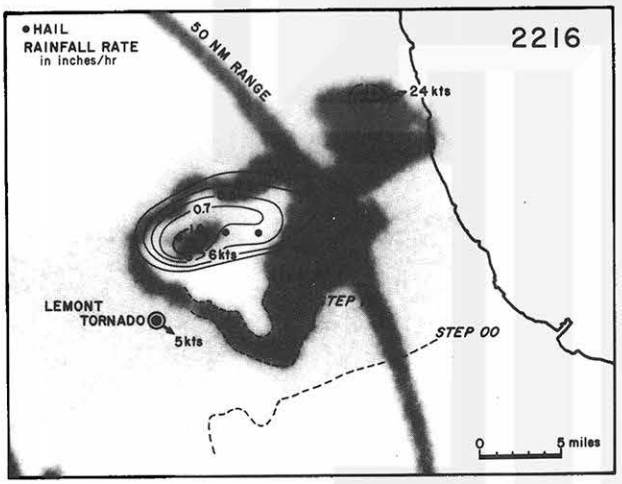

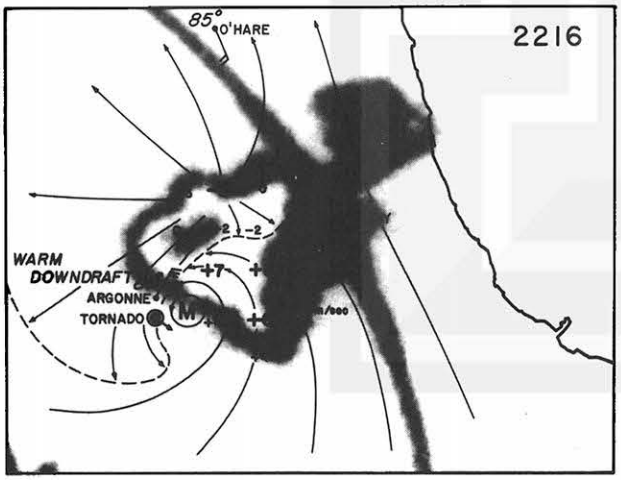

Fig. 16. Mesoanalyses of rainfall rate (above) and apparent vertical velocity at 2216Z, June 13, 1976.

At 2231Z when the Lemont tornado reached its F 4 (peak) intensity, the rain core still existed at the reflectivity center. The rainfall rate at the core was that expected from the mean S - R line, resulting in no apparent updraft or downdraft.

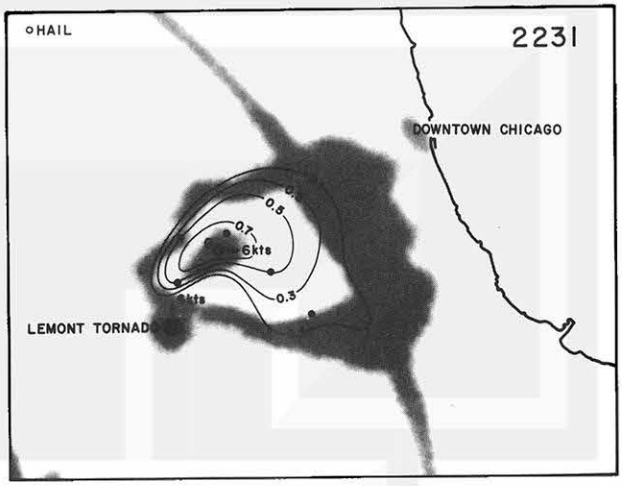

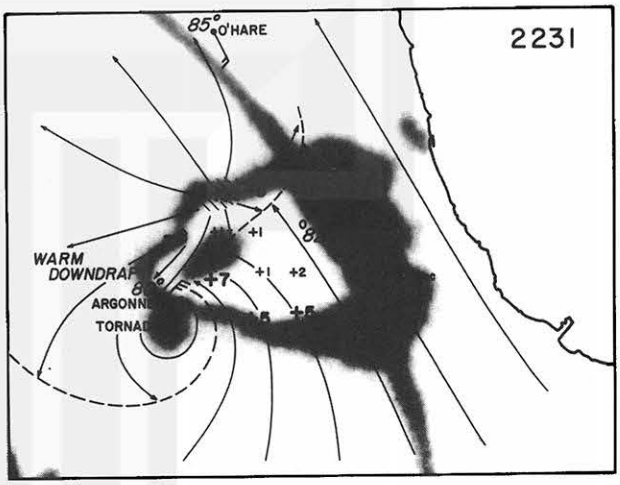

Fig. 17. Mesoanalyses of rainfall rate (above) and apparent vertical velocity at 2231Z, June 13, 1976.

The Argonne wind was still from the direction of the rain core. Temperature was a warm 80° F. A small center of strong apparent downdraft is seen near the north edge of the rain area.

It was not raining in the vicinity of the tornado which was seen as a large, circular echo, probably the result of airborne objects swirling in the tornado (Fujita, 1976).

At 2330 Z two major cores of rainfall were located over the reflectivity centers. Rain cores were moving at 7 to 9 kts in arbitrary directions, acting as giant obstacles against the westerlies.

Apparent downdraft in excess of 10 m/sec is seen to the south of the western rain core. At one station, 4 miles to the east of Argonne, the rainfall rate was so large that over 50 m/sec downdraft

would be required if the rate were to be explained by downdraft. A possible explanation would be horizontal transport of raindrops from a high-reflectivity source region to the east. A 30 kts cold outflow at Argonne supports the existence of a strong horizontal airflow.

If the calculated velocity exceeded 10 m/sec the existence of a horizontal flow from an area of higher reflectivity was assumed.

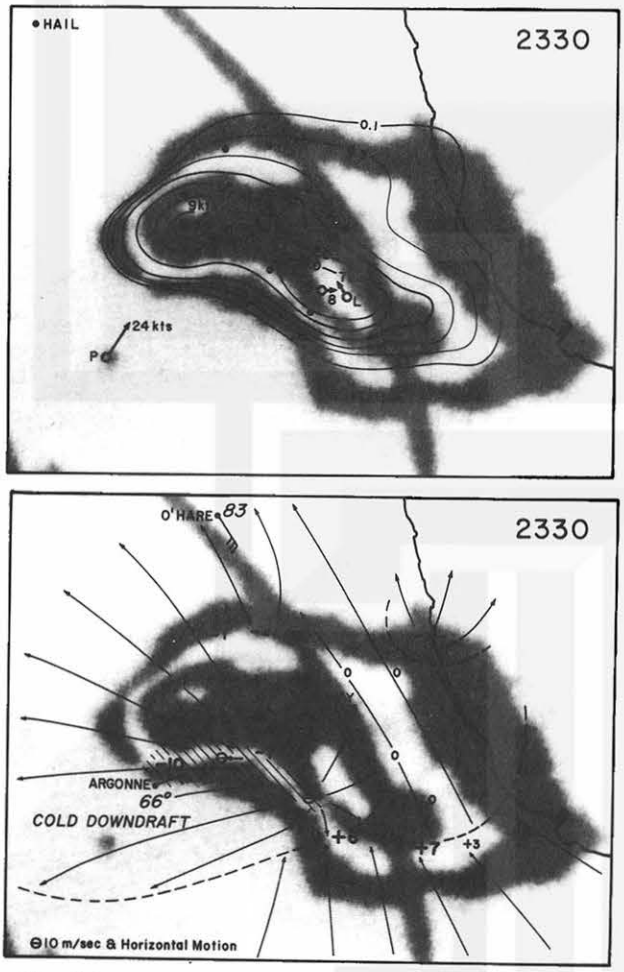

Fig. 18. Mesoanalyses of rainfall rate (above) and apparent vertical velocity at 2330Z; June 13, 1976.

At 0025 Z the rainfall patterns fit, more or less, the radar echo except near the southwest end of the echo where a wedge of rainfall pattern was seen. Isohyets there showed distinct "overflow" pattern, suggesting that raindrops were being thrown out toward the southwest by strong horizontal winds.

Evaluation of apparent draft velocities suggested the presence of large horizontal airflow at several stations near the wedge of rainfall. The radar echo pattern indicates the existence of strong circulations consistent with this analysis.

Rain core L was moving southwest at 10 kts against the steering flow. Three cores, N, R, and Q, were moving at 13 to 22 kts around the hook area which was acting as a giant blocking system.

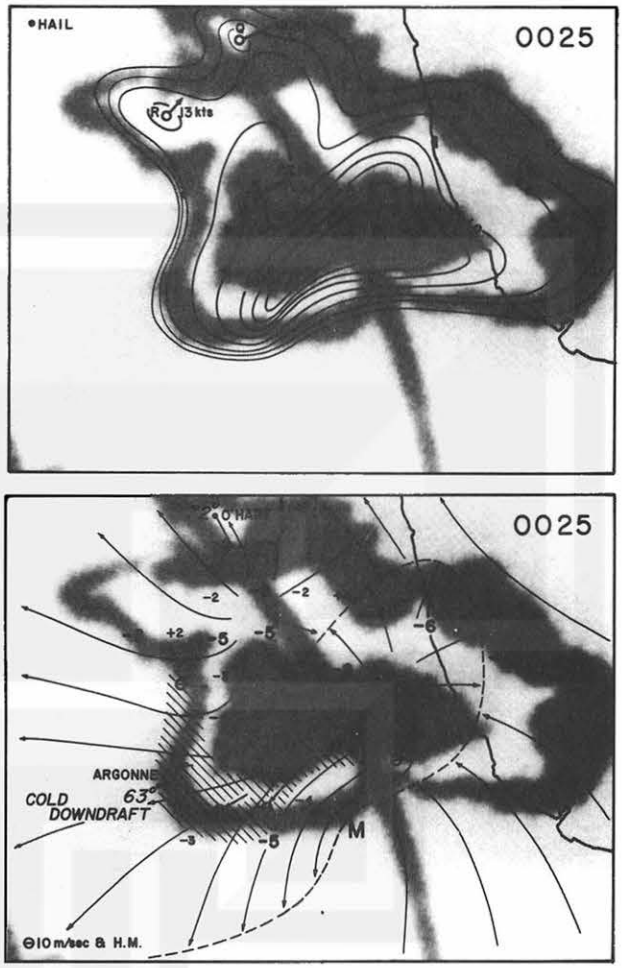

Fig. 19. Mesoanalyses of rainfall rate (above) and apparent vertical velocity at 0025Z, June 14, 1976.

8. CONCLUSIONS

Conclusions obtained through this research are

(a) The Chicago area rainstorm was a giant system causing up to 7 inches of rain.

(b) Areas of rain were extremely small relative to the satellite-viewed cloud.

(c) Blocking of rainstorm induced a wake cirrus and herringbone anvil.

(d) Cloud-top reflectivity above rain cores was either dark or bright.

(e) Reflectivity of hail was overshadowed by that of raindrops.

(f) Computations yielded airflows consistent with those expected in such a storm. Therefore, one should expect large deviations from mean Z - R relationships in storms with strong circulations.

Acknowledgement:-

The research performed at the University of Chicago has been supported by NOAA under Grant 04-4-158-1 and by NASA under Grant NGR 14-001-008.

The research performed at the Illinois State Water Survey has been supported by the National Science Foundation under Grant ENV 76-01447.

REFERENCES

Changnon, S. A., 1968: Surface models of hailstorms. Proc. Internation Conf. on Cloud Physics, Toronto, AMS, Boston, 478-482.

_____ and F. A. Huff, 1976: Chicago Hydrometeorological Area Project: A comprehensive new study of urban hydrometeorology. First Interim Report NSF ENV 76-01447, Ill. Water Survey, Urbana, 69 pp.

_____ and G. M. Morgan, 1976: The design of an experiment to suppress hail in Illinois. Bull 61, Ill. Water Survey, Urbana, 194 pp.

Fujita, T. T., 1974: Overshooting thunderheads observed from ATS and Learjet. SMRP Research Paper 117, 29 pp.

_____, 1976: Lemont-Argonne Tornado of June 13, 1976. SMRP Research Paper 144.

Gunn, R. and G. D. Kinzer, 1949: The terminal velocity of all for water droplets in stagnant air. J. Meteor., 6, 243-248.

Marshall, J. S. and W. McK. Palmer, 1948: The distribution of raindrops with size. J. Meteor., 5, 165-166.